

UC Davis

UC Davis Previously Published Works

Title

Supramolecular Assembly of Ag(I) Centers: Diverse Topologies Directed by Anionic Interactions

Permalink

<https://escholarship.org/uc/item/2qz2d1vf>

Journal

Crystal Growth & Design, 14(10)

ISSN

1528-7483

Authors

deBoer, TR
Chakraborty, I
Olmstead, MM
[et al.](#)

Publication Date

2014-10-01

DOI

10.1021/cg501175g

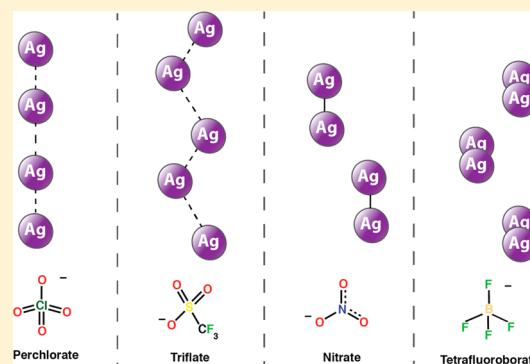
Peer reviewed

Supramolecular Assembly of Ag(I) Centers: Diverse Topologies Directed by Anionic Interactions

T. R. deBoer,[†] I. Chakraborty,[†] M. M. Olmstead,[‡] and P. K. Mascharak^{*,†}[†]University of California, Santa Cruz, 1156 High Street, Santa Cruz, California 95064, United States[‡]University of California, Davis, 1 Shields Avenue, Davis, California 95616, United States

Supporting Information

ABSTRACT: Ag(I)–Ag(I) interactions in supramolecular structures have been achieved through the use of structural support from the ligand frames. In structures involving simple ligands like pyridine, strong π – π interaction leads to spatial ordering of the individual $[\text{Ag}(\text{L})_2]^+$ units. In such structures anions also play a crucial role in dictating the final arrangement of the $[\text{Ag}(\text{L})_2]^+$ synthons. In order to determine whether the anions can solely dictate the arrangement of the $[\text{Ag}(\text{L})_2]^+$ synthons in the supramolecular structure, four Ag(I) complexes of 4-pyridylcarbinol (PyOH), namely, $[\text{Ag}(\text{PyOH})_2]\text{X}$ ($\text{X} = \text{NO}_3^-$ (1), BF_4^- (2), CF_3SO_3^- (3), and ClO_4^- (4)) have been synthesized and structurally characterized. Gradual transformation of the extended structures observed in 1–3 eventually merges into a unique linear alignment of the $[\text{Ag}(\text{PyOH})_2]^+$ units in 4 along the c axis, a feature that results in strong argentophilic interactions. Complex 4 is sensitive to light and is inherently less stable than the other three analogues. The structural variations in this set of extended assemblies are solely dictated by the anions, since π – π interaction between the substituted pyridine ligands is significantly diminished due to disposition of the $-\text{CH}_2\text{OH}$ substituent at the 4 position and H-bonding throughout the structure.



The complex combinations of molecular synthons have long been studied to establish design principles capable of dictating topologies, geometries, and packing arrangements of supramolecular structures.¹ Attempts to establish *predictable controls* over such structures have required the use of model systems that can be easily manipulated to probe discrete properties that contribute to extended packing of simple building units.^{2,3} While the design and construction of ligand frames has been the major strategy for fabricating infinite arrays of synthons,^{4,5} noncovalent interactions have also been observed to impart significant effects on the geometry and topology of coordination polymers. Because Ag(I) cationic complexes display flexible coordination geometries and are readily synthesized, they have commonly been utilized as building blocks of coordination polymers. Structures of the coordination polymers of such Ag(I) synthons can be tuned (a) by altering ligand geometry, rigidity, or functionality, (b) by exchanging the counterions, or (c) by altering the solvent system.⁵ Ag(I) centers have also been shown to exhibit metal–metal interactions that strongly influence the conductive and luminescent properties of an extended structure.

Closed shell d^{10} – d^{10} metallophilic interactions are known to afford multinuclear aggregates and three-dimensional networks with novel and diverse structures.⁶ Early examples of such metal–metal aggregates were predominantly derived from Au(I). Theoretically, ready formation of these aggregates was attributed to *contraction* of the 6s orbitals resulting in the admix

of 5d orbitals to effectively reduce the population of the 5d valence shell.⁷ In general, Ag–Ag (argentophilic) interactions are weaker than Au–Au, and are strongly dependent on the corresponding coordinated ligand frames. While ligand-mediated processes contribute to global supramolecular structure, intramolecular interactions also strongly dictate the microarchitecture and can have a profound influence on the physical properties of the polymeric system. One such example is $[\text{Ag}(2\text{-AMPDPN})\text{X}]$, (AMPDPN = 2-aminomethylpyridine-dipropionitrile, $\text{X} = \text{CF}_3\text{SO}_3^-$, ClO_4^- , and NO_3^-), where modulation of the counteranion grossly directs the structural topology from a three-coordinate one-dimensional ladder, to a four-coordinate one-dimensional ladder with Ag–Ag interactions, to a two-dimensional helical network, respectively.^{8,9}

In the present work, we report the synthesis and crystallographic characterization of analogous Ag(I) structures that vary only in the selected counteranion, namely, $[\text{Ag}(\text{PyOH})_2]\text{X}$ (where PyOH = 4-pyridylcarbinol and $\text{X} = \text{NO}_3^-$, BF_4^- , ClO_4^- , and CF_3SO_3^-). Crystallographic data reveal dramatic variations in the observed argentophilic interactions and global supramolecular structures with simple exchange of the counteranions in this series. This anion-dependent modulation was proposed previously by Lee and co-workers following the synthesis and

Received: August 5, 2014

Revised: September 3, 2014

Published: September 11, 2014

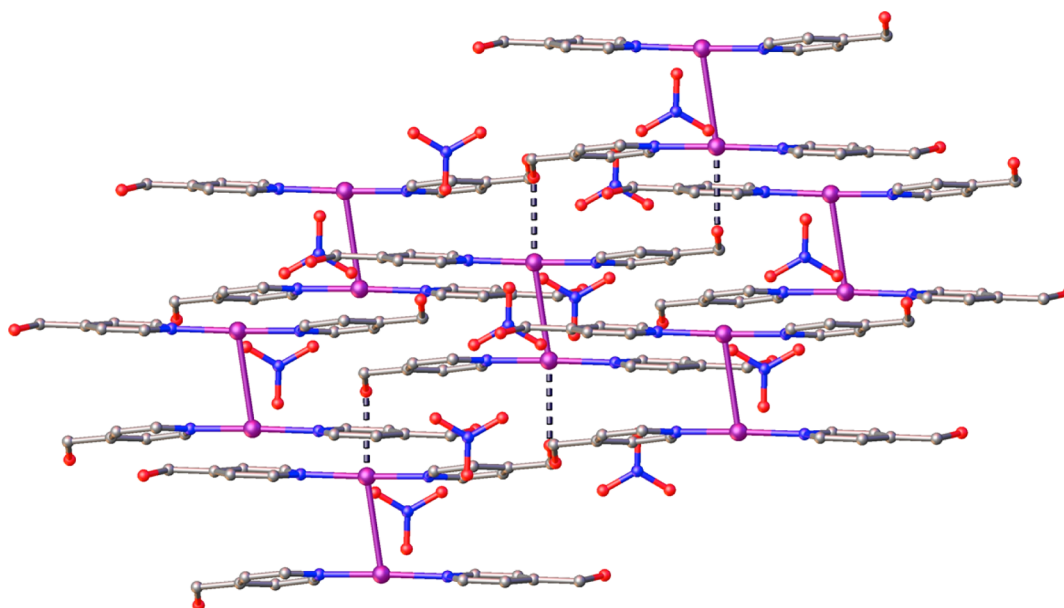


Figure 1. Crystal structure of **1** along the c axis (generated with the aid of the program OLEX2¹⁵).

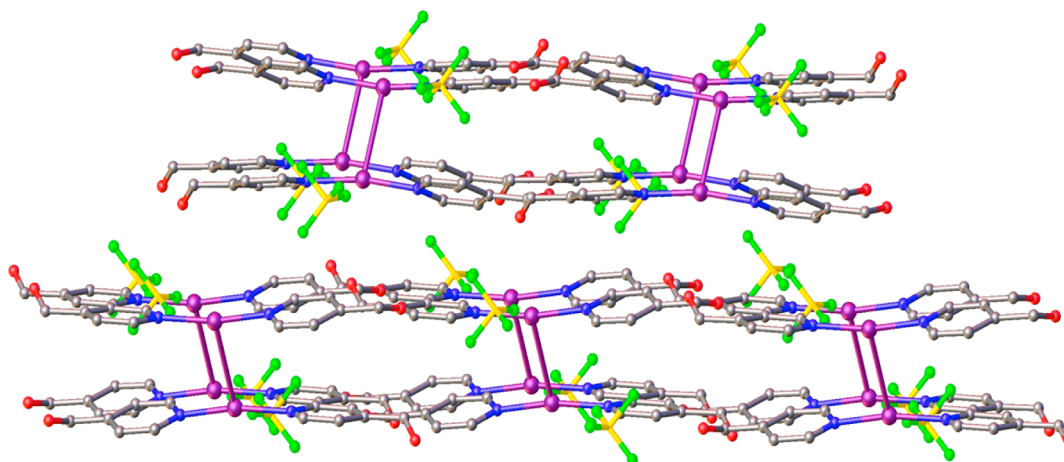


Figure 2. Crystal structure of **2** down the c axis (generated with the aid of the program OLEX2¹⁵).

characterization of three simple Ag(I) pyridine analogues that varied only in the counteranion ($[\text{Ag}(\text{Py})_2]\text{X}$, $\text{X} = \text{ClO}_4^-$, BF_4^- , and PF_6^-).¹⁰ In this set of Ag(I) coordination polymers, one-dimensional infinite chains of Ag(I) dimer units ($[\text{Ag}(\text{Py})_2]_2^{2+}$) were observed when a tetrahedral anion was chosen as the counterion (ClO_4^- and BF_4^-) while three-dimensional polymeric Ag(I) chains were noted when the octahedral anion PF_6^- was employed. Although the distinct argentophilic interactions were hypothesized to be driven by the geometry of the counteranion, crystallographic data highlighted strong π - π interactions between stacking pyridine ligands in the ClO_4^- and BF_4^- analogues (centroid-centroid distance of 3.569 and 3.541 Å, respectively), a feature capable of contributing to the Ag-Ag interactions observed in these structures. *To explore the possibility of a truly anion-driven argentophilic interaction, we have employed the pyridine derivative PyOH in the present work. This pyridine-based ligand contains a flexible terminal alcohol group capable of disrupting the π - π stacking of the pyridyl rings in addition to secondary interactions with the metal centers and/or the counteranions.*

Syntheses of $[\text{Ag}(\text{PyOH})_2]\text{NO}_3$ (**1**), $[\text{Ag}(\text{PyOH})_2]\text{BF}_4 \cdot \text{CH}_3\text{CN}$ (**2**), $[\text{Ag}(\text{PyOH})_2]\text{CF}_3\text{SO}_3$ (**3**), and $[\text{Ag}(\text{PyOH})_2]\text{ClO}_4$ (**4**) were achieved by addition of concentrated ethanolic solution of dry PyOH to rapidly stirred ethanolic (or acetonitrile) solution of the corresponding silver salt (AgNO_3 , AgBF_4 , AgClO_4 , and AgCF_3SO_3) (Supporting Information). After 1 h of stirring, white solid began to form in all reactions. The microcrystalline solids were collected after each solution was concentrated and cooled to 4 °C. Please refer to ref 16 for crystallographic data. Clear colorless diffraction quality blocks of **1** were obtained by vapor diffusion of diethyl ether into a methanolic solution of the silver complex at 4 °C. Similar crystallization procedure afforded clear blocks of **2**, thick plates of **3**, and thin needles of **4** within 24–72 h.

X-ray crystallographic analysis of **1**, **2**, **3**, and **4** (Supporting Information) revealed distinct Ag(I) topologies. In structure **1**, Ag(I) atoms are paired in discrete dimer units along the c axis (deviating 8.83° from the vertical axis) with a Ag-Ag distance of 3.2141(2) Å (Figure 1). The pyridyl nitrogen of the PyOH ligands linearly coordinates the Ag(I) center, and the aromatic moieties are near planar but display asymmetric interannular

torsional angles in the plane orthogonal to the Ag(I) dimer (0.5° and 6.8°). The Ag(I) dimers stack in a staggered fashion impeding long-range π -stacking of the aromatic ring systems. The terminal oxygen atoms of the PyOH ligands weakly interact with adjacent Ag(I) centers of the dimer, namely, $\text{Ag1}\cdots\text{O}_{\text{Ligand}}$ 2.794(5) Å and $\text{Ag2}\cdots\text{O}_{\text{Ligand}}$ 3.540(4) Å. The $\text{Ag}\cdots\text{O}$ interactions may contribute to the observed spatial orientation of the terminal alcohol groups (torsional angles 5.5° and 158°) that outcompete intermolecular H-bonding. The NO_3^- ions of **1** function to balance the charge of the complex and are embedded within the void spaces in between the dimer units. The NO_3^- counterion does not appreciably interact with the ligand units of the structure, but instead weakly coordinate to the Ag(I) centers through an oxygen (2.862(5) Å). Overall, the absence of strong intermolecular interactions between the ligand π -system or the terminal OH groups suggest that the structural topology observed in the extended structure of **1** is not guided by the PyOH ligand but by the NO_3^- counterion.

Exchange of the trigonal planar NO_3^- counterion with tetrahedral BF_4^- in **2** resulted in significant structural changes in addition to slightly longer Ag–Ag bond (3.3171 (1) Å). While planar NO_3^- traverses parallel to the Ag–Ag bonds of **1** with the N atom residing near the center of this bond (Ag–N 3.577(4) Å and Ag–N 3.468(4) Å, Figure 1), BF_4^- ions interact with only one of the Ag centers of the dimeric units in **2** (Ag–F 3.398(4) Å, Figure 2). Further, significant H-bonding between the F atoms of BF_4^- and the alcohol group of PyOH ligands (2.851(2) Å and 2.808(4) Å) in succession with $\text{Ag}\cdots\text{O}_{\text{PyOH}}$ interactions (3.615(3) Å) induces torsion of the pyridyl rings along the a – c plane that results in the near edge-on-edge orientation of the pyridyl rings of the dimer unit (Figure 2). The orientation of the PyOH ligands along the N–Ag–N axis does not appear to contribute significant destabilization or stabilization of the dimer units of structures **1** or **2**. In the NO_3^- analogue **1**, the methanol groups of the PyOH ligand are oriented in an *anti*-fashion, while in structure **2**, they exist in a *syn*-fashion. It may be expected that spatial arrangement of the OH groups of neighboring PyOH ligands in the dimeric units of **2** would promote H-bonding interactions that would enhance the argentophilicity of the Ag(I) centers. However, this was not observed presumably due to tilt of the pyridyl moieties.

The crystallographic structure of the triflate-containing complex **3** displays a zigzag orientation of Ag(I) atoms along the c axis, in a $\text{Ag1}-\text{Ag2}-\text{Ag1}'-\text{Ag2}'$ fashion, with $\text{Ag1}-\text{Ag2}$ and $\text{Ag2}-\text{Ag1}'$ distances of 3.546(4) and 3.885(4) Å, respectively (Figure 3, top). The PyOH ligands are linearly coordinated to the Ag(I) centers and are approximately planar. Examination of the structure along the c axis highlights the alternating units of $[\text{Ag}(\text{PyOH})_2]^+$ eclipsing each other (Figure 3, bottom). It has been established that anion-bridging interactions can play a significant role in long-range structural order, and the anions of **3** highlight this feature. The CF_3SO_3^- ions link neighboring zigzag units through H-bonding interactions of the anion with the PyOH groups of one chain (2.575(5) Å) and alternating $\text{Ag}\cdots\text{O}(\text{CF}_3\text{SO}_3^-)$ interactions of another (Figure 3, top). The spatial orientation of CF_3SO_3^- along the zigzag chain of Ag(I) centers mirrors that of NO_3^- in structure **1**. Alternating $\text{Ag}\cdots\text{S}_{\text{Triflate}}$ interactions (3.887(5) Å and 4.009(5) Å, respectively) are significantly weaker than the noncovalent $\text{Ag}\cdots\text{N}(\text{NO}_3)$ interaction observed in **1** possibly attributed to variability in close packing as a function of the

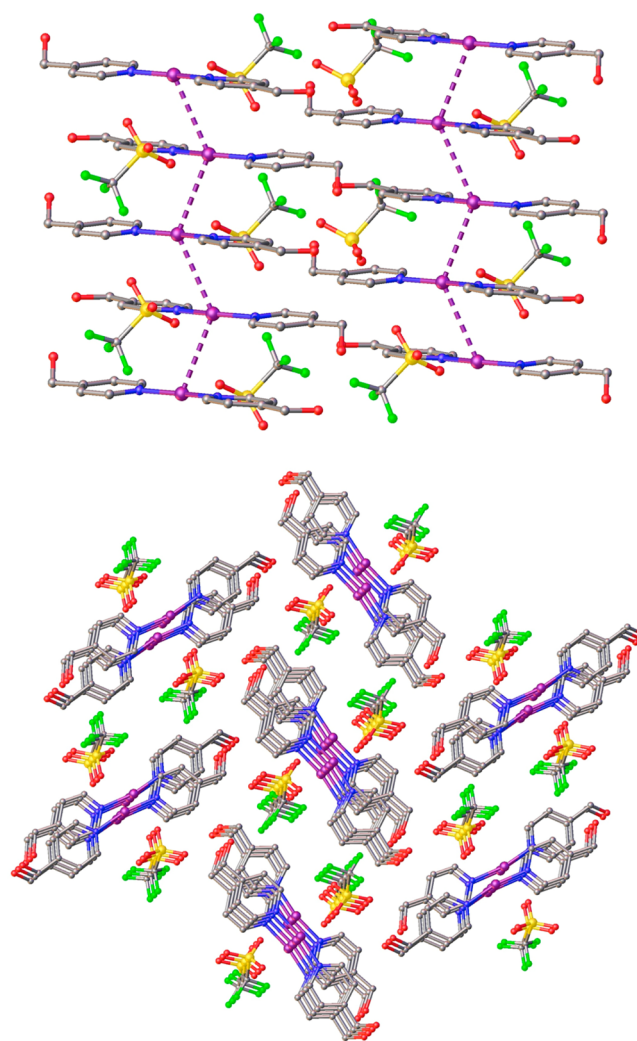


Figure 3. Crystal structure of **3** oriented along (top) and down (bottom) the c axis (generated with the aid of the program OLEX2¹⁵).

significant size disparity between the molecular volumes of the CF_3SO_3^- and NO_3^- ions (86.9 Å³ and 34 Å³, respectively).

In contrast to structures **1**, **2**, and **3**, structure **4** exhibits linear chains of Ag(I) centers stacked along the c axis, with alternating covalently linked Ag–Ag dimers (3.241(5) Å) and noncovalent $\text{Ag}\cdots\text{Ag}$ (3.462(5) Å) units (Figure 4, top) in a $\text{Ag3}-\text{Ag1}-\text{Ag2}-\text{Ag3}'-\text{Ag1}'-\text{Ag2}'$ fashion. The pyridyl rings of the $\text{Ag3}-\text{Ag1}-\text{Ag2}-\text{A3}'$ chains are staggered and exhibit distinct torsional angles, imposing nonplanar stacking of aromatic moieties in the a plane (centroid–centroid distances = 3.685 Å, 3.667 Å, and 3.743 Å, respectively). Examination of this catenated building block down the c axis highlights the asymmetry of the ligand appendages (Figure 4, bottom). Cross-section of this unit orthogonal to the aromatic rings through the Ag(I) chain accentuates this feature, and reveals a weak H-bond network established through the OH groups between adjacent units along the a – b plane. In addition, eclipsing ClO_4^- anions down the c axis between the stacked silver chains and the terminal alcohol groups of the contiguous $\text{Ag1}-\text{Ag2}-\text{Ag3}$ units exhibit an extensive bridging network that appears to drive the architecture of the extended structure (Figure 4, Top). Unlike the weak $\text{Ag}\cdots\text{O}(\text{NO}_3^-)$ interactions observed in the structure of **1**, there are 11 distinct $\text{Ag}\cdots\text{O}(\text{ClO}_4^-)$

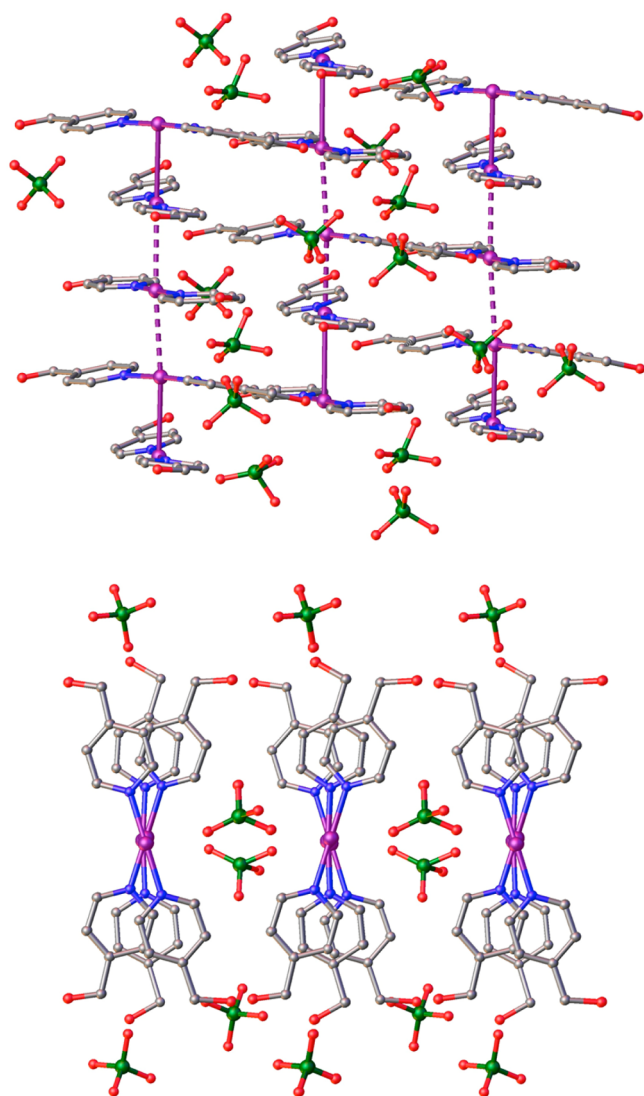


Figure 4. Crystal structure of **4** oriented along (top) and down (bottom) the *c* axis (generated with the aid of the program OLEX2¹⁵).

interactions with distances ranging from 2.706(4) to 3.553(5) Å.

It has been proposed that strong repulsive electrostatic interaction contributes to the instability of Ag–Ag bond formation, validating common ligand-supported strategies to push such argentophilic interactions.¹¹ Structures of the present Ag(I) complexes **1–4**, however, arise principally from interactions with the anions and H-bonding. Catenation of the Ag(I) atoms along the *c* axis is stabilized by the extended long-range noncovalent interactions in structure **4**. As a consequence, the delicate clear needles of **4** are grossly unstable and decompose when exposed to light, resulting in physical disfigurement and discoloration of the crystals. It has been shown that the effects of high-energy radiation on silver salts are markedly different between NO₃[−] and ClO₄[−].^{12,13} Observations indicate that the NO₃[−] group of AgNO₃ is primarily the electron gaining center, while exposure of silver perchlorate salts to high-energy radiation typically results in reduction of the Ag^I center to Ag⁰. Symons and co-workers illustrated this point using Ag(I) imidazole ClO₄[−] complex [Ag(Im)₂]ClO₄. Exposure of this complex to ⁶⁰Co γ -rays at 77

K resulted in the reduction of silver atoms within the (Ag⁺)₆ cluster.¹⁴

Results of the current work demonstrate that the change in the counteranion from NO₃[−] to BF₄[−] to CF₃SO₃[−] and finally to ClO₄[−] give rise to distinct structural topologies capable of imposing argentophilic interactions at Ag(I) centers of a simple coordination complex [Ag(PyOH)₂]⁺. Selection of 4-pyridyl-carbinol as the ligand deterred strong π – π interactions of the pyridyl moiety (a characteristic noncovalent interaction observed in [Ag(Py)₂]⁺ complexes) and allowed us to specifically probe the ability of anions to influence Ag–Ag interactions in supramolecular structures. In **1**, discrete Ag–Ag dimers are observed along the *c* axis with minimal intermolecular interactions between the ligand frames of the [Ag(PyOH)₂]⁺ units. Evolution of these discrete units toward an intermediate structure where silver atoms weakly interact in an extended semilinear fashion was achieved by employing CF₃SO₃[−] in structure **3**. Alignment of the Ag(I) centers to form linear chains that feature argentophilic interactions was finally achieved in structure **4**, where the ClO₄[−] was selected as the counteranion. The counterions in these complexes dictate both the architecture of the polymeric structures and the Ag–Ag interactions. In this context, the present results are distinct given the extensive number of reports on ligand-supported Ag–Ag interactions, where designed ligands are commonly required to attain the supramolecular structures.

■ ASSOCIATED CONTENT

📄 Supporting Information

Materials and methods, spectral and analytical data, and tables of H-bonding and other short contacts for complexes **1–4**. This material is available free of charge via the Internet at <http://pubs.acs.org>.

Accession Codes

CCDC 1007177–1007179, 1013954.

■ AUTHOR INFORMATION

Corresponding Author

*E-mail: Pradip@ucsc.edu. Telephone: (831) 459-4251. FAX: (831) 459-2935.

Notes

The authors declare no competing financial interest.

■ ACKNOWLEDGMENTS

Financial support from the NSF grant DMR-140933 is gratefully acknowledged. TRdB was supported by GM-58903.

■ REFERENCES

- (1) Desiraju, G. R. *J. Am. Chem. Soc.* **2013**, *135*, 9952.
- (2) Fabbrizza, L.; Poggi, A., Eds. In *Transition Metals in Supramolecular Chemistry*; VCH, 1994.
- (3) Bosch, E.; Barnes, C. L. *Inorg. Chem.* **2002**, *41*, 2543.
- (4) Jin, C.-M.; Chen, Z.-F.; Mei, H.-F.; Shi, X.-K. *J. Mol. Struct.* **2009**, *921*, 58.
- (5) Feazell, R. P.; Carson, C. E.; Klausmeyer, K. K. *Inorg. Chem.* **2006**, *45*, 2635.
- (6) Lin, Y.-Y.; Lai, S.-W.; Che, C.-M.; Cheung, K.-K.; Zhou, Z.-Y. *Organometallics* **2002**, *21*, 2275.
- (7) Singh, K.; Long, J. R.; Stravropoulos, P. *J. Am. Chem. Soc.* **1997**, *119*, 2942.
- (8) Kang, Y.; Lee, S. S.; Park, K.-M.; Lee, S. H.; Kang, S. O.; Ko, J. *Inorg. Chem.* **2001**, *40*, 7027.

(9) Hannon, M. J.; Painting, C. L.; Plummer, E. A.; Childs, L. J.; Alcock, N. W. *Chem.—Eur. J.* **2002**, *8*, 2225.

(10) Chen, C. Y.; Zeng, J. Y.; Lee, H. M. *Inorg. Chim. Acta* **2007**, *360*, 21.

(11) Zheng, S.-L.; Volkov, A.; Nygren, C. L.; Coppens, P. *Chem.—Eur. J.* **2007**, *13*, 8583.

(12) Mosley, W. C.; Moulton, W. G. *J. Chem. Phys.* **1965**, *43*, 1207.

(13) Symons, M. C. R.; Brown, D. R.; Eastland, G. W. *Chem. Phys. Lett.* **1979**, *61*, 92.

(14) Eastland, G. W.; Mazid, M. A.; Russell, D. R. M. C. R.; Symons, M. C. R. *J. Chem. Soc., Dalton Trans.* **1980**, 1682.

(15) Dolomanov, O. V.; Bourhis, L. J.; Gildea, R. J.; Howard, J. A. K.; Puschmann, H. *J. Appl. Crystallogr.* **2009**, *42*, 339–341.

(16) Metal perchlorates are hazardous and may explode upon heating or rapid mechanical force. Crystal data for **1** ($C_{12}H_{14}AgN_3O_5$): $M_r = 388.13$, triclinic, space group $P\bar{1}$, $a = 9.0424(14)$ Å, $b = 9.4680(15)$ Å, $c = 9.6852(15)$ Å, $\alpha = 61.961(2)^\circ$, $\beta = 82.929(2)^\circ$, $\gamma = 66.879(2)^\circ$, $V = 671.14(18)$ Å³, $Z = 2$, $\rho = 1.921$ g cm⁻³, $\mu = 1.528$ mm⁻¹, $F(000) = 388$, 10788 reflections measured, 3792 unique ($R_{int} = 0.0212$), $R1 = 0.0203$, $wR2 = 0.0469$ [$I > 2\sigma(I)$], GooF = 1.048. Crystal data for **2**•CH₃CN ($C_{14}H_{17}AgBF_4N_3O_2$): $M_r = 451.97$, monoclinic, space group $P2_1/n$, $a = 10.8154(10)$ Å, $b = 13.8641(12)$ Å, $c = 12.2098(11)$ Å, $\beta = 100.6320(10)^\circ$, $V = 1799.4(3)$ Å³, $Z = 4$, $\rho = 1.668$ g cm⁻³, $\mu = 1.171$ mm⁻¹, $F(000) = 896$, 13671 reflections measured, 2703 unique ($R_{int} = 0.0175$), $R1 = 0.0752$, $wR2 = 0.2412$ [$I > 2\sigma(I)$], GooF = 1.081. Crystal data for **3** ($C_{13}H_{14}AgN_2O_3F_3S$): $M_r = 475.19$, monoclinic, space group $P2_1/c$, $a = 6.5938(8)$ Å, $b = 22.968(3)$ Å, $c = 11.1850(13)$ Å, $\beta = 102.940(2)^\circ$, $V = 1650.9(3)$ Å³, $Z = 4$, $\rho = 1.912$ g cm⁻³, $\mu = 1.407$ mm⁻¹, $F(000) = 944$, 36733 reflections measured, 4436 unique ($R_{int} = 0.0319$), $R1 = 0.0315$, $wR2 = 0.0585$ [$I > 2\sigma(I)$], GooF = 1.076. Crystal data for **4** ($C_{12}H_{14}AgN_2O_6Cl$): $M_r = 425.57$, monoclinic, space group $C2/c$, $a = 10.1508(12)$ Å, $b = 14.5838(17)$ Å, $c = 31.448(4)$ Å, $\beta = 90.250(2)^\circ$, $V = 4655.4(9)$ Å³, $Z = 12$, $\rho = 1.822$ g cm⁻³, $\mu = 1.500$ mm⁻¹, $F(000) = 2544$, 30925 reflections measured, 5323 unique ($R_{int} = 0.0302$), $R1 = 0.0952$, $wR2 = 0.2440$ [$I > 2\sigma(I)$], GooF = 1.113.